

¹³C isotopic ratios of HC₃N on Titan measured with ALMA

TAKAHIRO IINO,¹ KOTOMI TANIGUCHI,² HIDEO SAGAWA,³ AND TAKASHI TSUKAGOSHI²

¹*Information Technology Center, The University of Tokyo, 2-11-16 Yayoi, Bunkyo, Tokyo 113-8658, Japan*

²*National Astronomical Observatory of Japan, 2-21-1 Osawa, Mitaka, Tokyo 181-8588, Japan*

³*Faculty of Science, Kyoto Sangyo University, Motoyama, Kamigamo, Kita-ku, Kyoto 603-8555, Japan*

(Received; Revised; Accepted)

ABSTRACT

We present the first determination of the abundance ratios of ¹³C substitutions of cyanoacetylene (HC₃N), [H¹³CCCN]:[HC¹³CCN]:[HCC¹³CN] in Titan’s atmosphere measured using millimeter-wave spectra obtained by the Atacama Large Millimeter-submillimeter Array. To compare the line intensities precisely, datasets which include multiple molecular lines were extracted to suppress effects of Titan’s environmental conditions and observation settings. The [HC¹³CCN]:[HCC¹³CN] and [H¹³CCCN]:[HCC¹³CN] ratios were obtained from 12 and 1 selected datasets, respectively. As a result, nearly the uniform [H¹³CCCN]:[HC¹³CCN]:[HCC¹³CN] abundance ratios as 1.17 (±0.20) : 1.09 (±0.25) : 1 (1σ) were derived, whereas previously reported ratios for interstellar medium (ISM) have shown large anomalies that may be caused by ¹³C concentrations in precursors. The result obtained here suggests that ¹³C concentration processes suggested in the ISM studies do not work effectively on precursors of HC₃N and HC₃N itself due to Titan’s high atmospheric temperature and/or depletion of both ¹³C and ¹³C⁺.

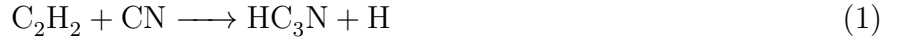
Keywords: planetary atmosphere — ALMA — submillimeter

1. INTRODUCTION

The ¹³C substituted species of cyanoacetylene (HC₃N), namely, H¹³CCCN, HC¹³CCN and HCC¹³CN, have been discovered in various interstellar media (ISM), and are known to exhibit large isotopic anomalies that HCC¹³CN and/or H¹³CCCN show high ¹³C concentrations (Takano et al. 1998; Taniguchi et al. 2016; Araki et al. 2016; Taniguchi et al. 2017). Such anomalies are considered to be due to the ¹³C concentrations on the precursors of HC₃N such as CN and C₂H (Furuya et al. 2011; Taniguchi et al. 2019), and give us important information on the environments and possible chemical reactions in the ISM.

HC₃N is also present on Saturn’s largest moon, Titan, and was first detected in the atmosphere by the Voyager 1 spacecraft (Kunde et al. 1981). The main production pathway of HC₃N was expected

as follows:



Since then, a number of in-situ, ground- and space-based observations have been performed to illustrate the spatial and time variation of HC_3N along with other nitriles and hydrocarbons (Hidayat et al. 1997; Coustenis et al. 1998, 2003; Gurwell 2004; Coustenis et al. 2007, 2010; Cordiner et al. 2014; Coustenis et al. 2016, 2018; Thelen et al. 2019).

Adding to Reaction 1, a following reaction of C_2H radical with HNC (Loison et al. 2015) possibly produces a portion of HC_3N because HNC is present in the upper stratosphere (Moreno et al. 2011; Cordiner et al. 2014).



In turn, due to the extremely high reaction barrier, the reaction of C_2H with HCN, an isomer of HNC, does not work effectively. Thus, Reaction 2 is the only reaction to produce HC_3N from C_2H radical.

Two precursor radicals of HC_3N , namely CN and C_2H , are important for the HC_3N production along with the reaction counterparts, C_2H_2 and HNC. They are easily produced by the photo-dissociation HCN and C_2H_2 molecules, and their expected abundances are ~ 10 ppb at 1000 km (Lavvas et al. 2008).

As for the ISM, ^{13}C substitutions of HC_3N have also been detected on Titan. The first observational result was reported by Jennings et al. (2008) using infrared spectra obtained with the Composite Infrared Spectrometer on-board Cassini spacecraft. Spectral emissions of the three isotopologues were clearly detected, whereas the HC^{13}CCN and HCC^{13}CN lines were blended. Using the H^{13}CCCN and HC_3N lines, the $^{12}\text{C}/^{13}\text{C}$ ratio was measured to be 79 ± 17 , which is consistent with that measured in HCN (70–120: Hidayat et al. (1997), 132 ± 25 or 108 ± 20 : Gurwell (2004), 89.8 ± 2.8 : Molter et al. (2016)) and C_2H_2 (84.8 ± 3.2 : Nixon et al. (2012)). A recent submillimeter spectroscopy using ALMA succeeded in the detection of H^{13}CCCN with a high S/N ratio along with HCCC^{15}N (Cordiner et al. 2018), although the $^{12}\text{C}/^{13}\text{C}$ value was not determined for HC_3N .

In this study, we report the first observational determination of the relative ^{13}C carbon isotopic ratios of three isotopologues of HC_3N , namely $[\text{H}^{13}\text{CCCN}]:[\text{HC}^{13}\text{CCN}]:[\text{HCC}^{13}\text{CN}]$ on Titan by analyzing a large dataset obtained by ALMA. The result enables us to compare the chemical environment of Titan with that of the ISM.

2. ANALYSIS

2.1. Data selection

Since Titan is often used as a calibrator of ALMA, a large amount of observation data of Titan is available in the ALMA archive. We calibrated and imaged all of the archived observational data of Titan that were available as of January 2020. The details of the calibration and imaging procedure were as described in our previous paper that analyzed nitrogen isotopic ratio of CH_3CN on Titan (Iino et al. 2020).

Spectral lines of the isotopologues of HC_3N are often observed by ALMA by chance because their pure rotational transitions appear every ~ 10 GHz. To measure the line intensities precisely, we have chosen spectral windows (SPW) that observed multiple isotopologues simultaneously. The usage of the data in the same SPW suppresses the systematic uncertainties arising from the differences in the observation configurations such as the synthesized beam size and absolute flux calibration, and

Titan’s environmental conditions such as the horizontal and vertical distribution of HC_3N and the atmospheric structure. To measure the line intensities that have a narrow (~ 1.5 MHz) line-width, SPW that have a high frequency resolution of < 2 MHz were chosen. The frequency difference between HC^{13}CCN and HCC^{13}CN that share the same rotational state J is no more than 20 MHz because they have a very similar rotational constant B . Thus, in most cases, they are observed in the same SPW. In turn, since the rotational constant of H^{13}CCCN is $\sim 2\%$ smaller than those of HC^{13}CCN and HCC^{13}CN , the number of SPW including three lines was smaller than that includes HC^{13}CCN - HCC^{13}CN pair.

As an important phenomenon, Titan’s trace gases including HC_3N and its precursors, C_2H_2 and HCN , are known to exhibit large spatial and time variations. The analyzed period, from 2012 to 2015, is a season of northern summer, when increase and decrease of trace species have been observed by Cassini and ALMA for southern and northern hemispheres, respectively (Cordiner et al. 2015; Thelen et al. 2019; Cordiner et al. 2019; Coustenis et al. 2018).

To decrease the effect of such data-to-data variability of the HC_3N spatial distribution, disk-averaged spectra were extracted from the imaged cube fits with a $0.''4$ radius circle which is large enough to cover the entire disk of Titan for all of the analyzed datasets.

The baseline structure of the spectra was attempted to be removed using polynomial fitting method, while the effect was very limited. For the line intensity measurement, spectral intensities within a range of ± 1 MHz from the line center were integrated. Noise level was measured in the line-free region and multiplied by \sqrt{n} where n is the number of averaged channel. After extracting 29 SPW which include multiple emission lines, SPW that exhibit high S/N ratio as > 4 were chosen for the intensity ratio measurement analysis.

The number of selected SPW including HC^{13}CCN - HCC^{13}CN and H^{13}CCCN - HCC^{13}CN pairs obtained with high S/N ratio were 12 and 1, respectively. Observation parameters of the selected SPW are summarized in Table 1. The rotational state transitions corresponding to 217, 226, 235, 244 and 271 GHz bands were $J = 24-23$, $25-24$, $26-25$, $27-26$ and $30-29$, respectively. For an selected H^{13}CCCN - HCC^{13}CN pair, they have different transition of $J=35-34$ and $34-33$ for H^{13}CCCN and HCC^{13}CN , respectively. Most of the bands are of the ALMA Band 6, except for 308 GHz of the Band 7. The project code 2015.1.00512.S data has a long observation time by concatenating short observation time data to improve the S/N ratio.

Figures 1 and 2 show the obtained spectra for each pair. The HC^{13}CCN and HCC^{13}CN lines are plotted in the same panels in Figure 1 due to small differences in frequency, while the lines for H^{13}CCCN and HCC^{13}CN are over-plotted in Figure 2. For H^{13}CCCN including data, as shown in Figure 2, since the HC^{13}CCN line was blended with a Ethyl Cyanide ($\text{C}_2\text{H}_5\text{CN}(36_{1,36} - 35_{1,35})$) line, only the HCC^{13}CN line was used for the intensity comparison. Note that the detection of $\text{C}_2\text{H}_5\text{CN}$ with ALMA was reported previously (Cordiner et al. 2015).

In Titan’s atmosphere, the chemical processes associated with HC_3N vary with altitude, with ion chemistry being dominant at high altitudes and neutral chemistry at low altitudes. Previous ALMA observation study (Thelen et al. 2019) derived an altitude range where HC_3N ($J=35-34$) is sensitive by the radiative transfer analysis of the disk averaged spectra. The optically thick line core region of ± 2 MHz from the line center probes at the ~ 800 km high altitude region, whereas wings has sensitivity at 150 km, where HC_3N shows abundance peaks in the high latitude regions. Because the

obtained intensities of isotopomer lines analyzed in our study are quite weaker than that of HC_3N line, we infer that the isotopomer lines have sensitivity at the lower stratosphere.

2.2. Abundance ratio calculation

To calculate the abundance ratios for the two pairs of isotopologues, as described methods below, we compared the measured integrated line intensities instead of retrieving the vertical abundance using radiative transfer method. Since they share similar vertical abundance, optical depth and the same temperature profile, their relative abundance can be derived with a proper consideration of the difference of the rotational transitions between the two isotopologues. In addition, optically thin molecular lines enable us to assume that the measured intensity is proportional to the optical depth. This method was also applied to the previous $[\text{H}^{13}\text{CCCN}]:[\text{HCCC}^{15}\text{N}]$ measurement using ALMA observation result (Cordiner et al. 2018). Because we did not need to consider the effect of the difference of beam size, temperature profile and three-Dimensional distribution of HC_3N , the only effect on the line intensity that was estimated and applied was the difference in spectroscopic parameters with respect to the stratospheric temperature. For the calculation of the parameters relating to opacity such as the partition function and population, the equations used were those listed in the appendix of Turner (1991) and Iino et al. (2014). Line parameters such as the Einstein coefficient A_{ul} , the lower state energy E_l and the rotational constant B , were obtained from the NASA JPL catalogue (Pickett et al. 1998). The considered excitation temperatures were from 140 to 180 K under the assumption of the local temperature equilibrium condition.

For the $\text{HC}^{13}\text{CCN} - \text{HCC}^{13}\text{CN}$ pair, the evaluation was simple because they share the same rotational state J . For the range of analyzed rotational transitions, the line intensity difference between HC^{13}CCN and HCC^{13}CN was estimated to be less than 0.02% for the modeled temperature range. The only exception was the $J=24-23$ transition, where HCC^{13}CN has three hyperfine splitting lines. In this case, the line intensities of three transitions were simply integrated. As a result, the line intensity difference for the $J=24-23$ pair was determined to be $\sim 0.2\%$. Thus, considering the line intensity difference between two isotopologues and optically thin line intensities, for all the $\text{HC}^{13}\text{CCN} - \text{HCC}^{13}\text{CN}$ pair, we used the integrated line intensity ratios as the abundance ratio. The derived $[\text{HC}^{13}\text{CCN}]/[\text{HCC}^{13}\text{CN}]$ ratios are shown in the rightmost column of Table 1. Figure 3 shows a histogram of the obtained $[\text{HC}^{13}\text{CCN}]/[\text{HCC}^{13}\text{CN}]$ ratio. Any fractionation relating to the rotational transition was found. The averaged mean value is 1.09 with a standard deviation of 0.25. Since the time variation of the isotopic ratios are beyond the scope of this paper, we simply average the data taken from 2012 to 2015 epoch.

For the $\text{H}^{13}\text{CCCN} - \text{HCC}^{13}\text{CN}$ pair, taking into account the different rotational states, it was determined that $\text{HCC}^{13}\text{CN}(J=34-33)$ has a 6.4% higher intensity than $\text{H}^{13}\text{CCCN}(J=35-34)$ in average under the assumed excitation temperature range. With this correction, we found the abundance ratio of $[\text{H}^{13}\text{CCCN}]/[\text{HCC}^{13}\text{CN}]$ to be 1.17 ± 0.20 . Note that this error was determined from the noise level of single spectrum.

3. DISCUSSION

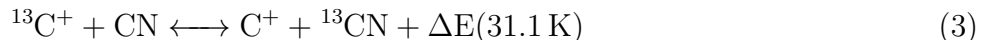
The measured $[\text{H}^{13}\text{CCCN}]:[\text{HC}^{13}\text{CCN}]:[\text{HCC}^{13}\text{CN}]$ ratios on Titan are nearly uniform within their errors. The ratios do not show the large anomalies as reported by the ISM observations that HCC^{13}CN and/or H^{13}CCCN show 35–110 and 20% higher abundance than the others, respectively (Takano et al. 1998; Araki et al. 2016; Taniguchi et al. 2016, 2017). Assuming that no time variation of $^{12}\text{C}/^{13}\text{C}$

ratio is present since the previous observation, the result indicates that the $^{12}\text{C}/^{13}\text{C}$ ratios on three isotopologues are same as 79 ± 17 that measured on H^{13}CCCN (Jennings et al. 2008). Below, the derived results are discussed from two viewpoints: ^{13}C concentration on HCC^{13}CN and H^{13}CCCN . The obtained absence of carbon fractionation process on Titan is possibly explained by the environmental difference such as atmospheric temperature between Titan and the ISM, and may constrain chemical reactions present in Titan’s middle and upper atmosphere.

3.1. HCC^{13}CN concentration

Assuming the main HC_3N production as Reaction 1, in case of HCC^{13}CN concentration exists, ^{13}C concentrations on CN and/or its precursor are greater than that in reaction counterparts, C_2H_2 , whose $^{12}\text{C}/^{13}\text{C}$ ratio was determined to be 84.8 ± 3.2 using the infrared spectra obtained by the Cassini spacecraft (Nixon et al. 2008). A main production pathway of CN is a photo-dissociation of HCN (Loison et al. 2015). The other pathway, a photo-dissociation of C_2N_2 , is negligible because the abundance is below 1–0.1% of HCN. The most recent ALMA observation reported that no significant ^{13}C concentration in HCN (89.8 ± 2.8 : Molter et al. (2016)) in relative to C_2H_2 . Thus, if exists, ^{13}C concentration on CN occurs after the photolysis of HCN.

An ion-molecule isotope exchange process between $^{13}\text{C}^+$ and CN has been proposed for exothermic ^{13}CN concentration process for interstellar clouds as follows (Colzi et al. 2020):

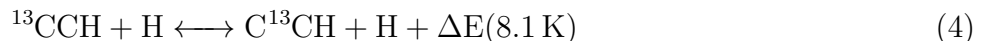


Reaction 3 likely causes HCC^{13}CN enrichment in some ISM, especially in low-temperature conditions ($\sim 10 \text{ K}$) (Takano et al. 1998). However, Reaction 3 does not seem to work effective on Titan’s relatively higher atmospheric temperature (140 – 180 K in the stratosphere) than interstellar, because the backward reaction of Reaction 3 can proceed and suppress the isotopic fractionation of CN in such high temperature environment.

The other scenario is relating to abundance of $^{13}\text{C}^+$ ion. Vuitton et al. (2007) calculated C^+ number density as $1.4\times 10^{-2} \text{ cm}^{-3}$ considering mas spectral measurement result. The calculated density is smaller than other major ions such as CH_2^+ , CH_3^+ , CH_5^+ , N^+ and so on, thus the Reaction 3 may not work effective to concentrate ^{13}C on CN and subsequently HC_3N .

3.2. H^{13}CCCN concentration

Reaction 2 is the only pathway to produce HC_3N from C_2H radical. Because C_2H_2 , a precursor of C_2H , is a symmetric carbon molecule, an anomaly between H^{13}CCCN and HC^{13}CCN is caused by the abundance difference between C^{13}CH and ^{13}CCH . In the ISM, the anomaly is possibly due to the isotope exchange reaction to achieve ^{13}C concentration on C^{13}CH as follows (Furuya et al. 2011):



Similar to the case of Reaction 3, forward reaction of Reaction 4 is considered to be active only in low temperature environment such as the starless cores. In case of Titan, Reaction 4 is not expected to work for concentration of C^{13}CH due to the high temperature condition. In addition, because of low HNC abundance (Moreno et al. 2011; Cordiner et al. 2014), contribution of the Reaction 2 for HC_3N production may be negligible.

4. SUMMARY AND FUTURE PROSPECT

We have detected the presence of all three ^{13}C substituted species of HC_3N , namely, H^{13}CCCN , HC^{13}CCN and HCC^{13}CN , in Titan’s atmosphere using observational data from ALMA archive. The statistically derived $[\text{HC}^{13}\text{CCN}]/[\text{HCC}^{13}\text{CN}]$ value was determined to be 1.09 ± 0.25 , whereas that of measured in starless dark clouds and low-mass star forming regions were previously reported to exceed the present error. Additionally, $[\text{H}^{13}\text{CCCN}]/[\text{HCC}^{13}\text{CN}]$ was found to be 1.17 ± 0.20 , although this result is less reliable than that for $[\text{HC}^{13}\text{CCN}]/[\text{HCC}^{13}\text{CN}]$ because of a single pair detection. For both cases, no significant ^{13}C concentration in HC_3N was detected, which differs from most of the ISM cases.

The large environmental difference with ISM is the high atmospheric temperature environment of Titan. A recent ALMA temperature measurement revealed that the measured stratospheric temperature above 100 km is at least 130 K, and reaches 180 K at 300 km (Thelen et al. 2018). These temperatures are quite higher than that expected in the ISM as 10 K (Taniguchi et al. 2019). In such a cold region with temperatures around 10 K, the barrierless and exothermic isotopic exchange reactions, Reactions 3 and 4, which have been considered to cause fractionation on HC_3N , are driven by the differences in the zero point energy. On the other hand, in a high temperature environment, such as Titan’s stratosphere and mesosphere, the backward reactions of Reactions 3 and 4 can proceed to suppress the isotopic fractionation in the precursors of HC_3N and HC_3N itself.

Recently, similar to the case of Titan, Taniguchi et al. (2021) reported uniform carbon isotopic ratios of HC_3N around a massive young star objects. They proposed that HC_3N is mainly produced via HC_3NH^+ ion, which has complicated formation pathway, which introduces more complicated pathways of HC_3N formation pathways and thus the entire HC_3N isotopic ratios would be affected by other reactions than Reactions 3 and 4. In addition to Reactions 1 and 2, a recent study suggested that the photo-dissociation of $\text{C}_2\text{H}_3\text{CN}$ and H-atom addition to HC_4N_2 may produce HC_3N (Vuitton et al. 2019). For the total understanding of Titan’s isotopic fractionation processes, such ion-relating reactions and newly proposed neutral reactions should be investigated.

Similar to Reaction 3, new exchange reactions of ^{13}C and $^{13}\text{C}^+$ with C-bearing species are proposed by recent publications (Colzi et al. 2020; Loison et al. 2020). These newly proposed reactions may induce ^{13}C concentrations in C-bearing species, in particular if ^{13}C and $^{13}\text{C}^+$ are abundant which is unlikely in Titan atmosphere. Our result, together with the previously reported non-concentration of ^{13}C in C-bearing species on Titan such as CH_4 , C_2H_2 , HCN , HC_3N and CO , may be interpreted as the consequence of ^{13}C and $^{13}\text{C}^+$ depletion.

This study makes use of the ALMA data listed in the table 1. ALMA is a partnership of ESO (representing its member states), NSF (USA) and NINS (Japan), together with NRC (Canada), MOST and ASIAA (Taiwan), and KASI (Republic of Korea), in cooperation with the Republic of Chile. The Joint ALMA Observatory is operated by ESO, AUI/NRAO and NAOJ. This work was supported by grants from the Telecommunications Advancement Foundation (TI), the Japan Society for the Promotion of Science (JSPS) Kakenhi (17K14420, 19K14782, 20K14523, 20K04046 and 20K04017) and the Astrobiology Center Program of National Institutes of Natural Sciences (NINS).

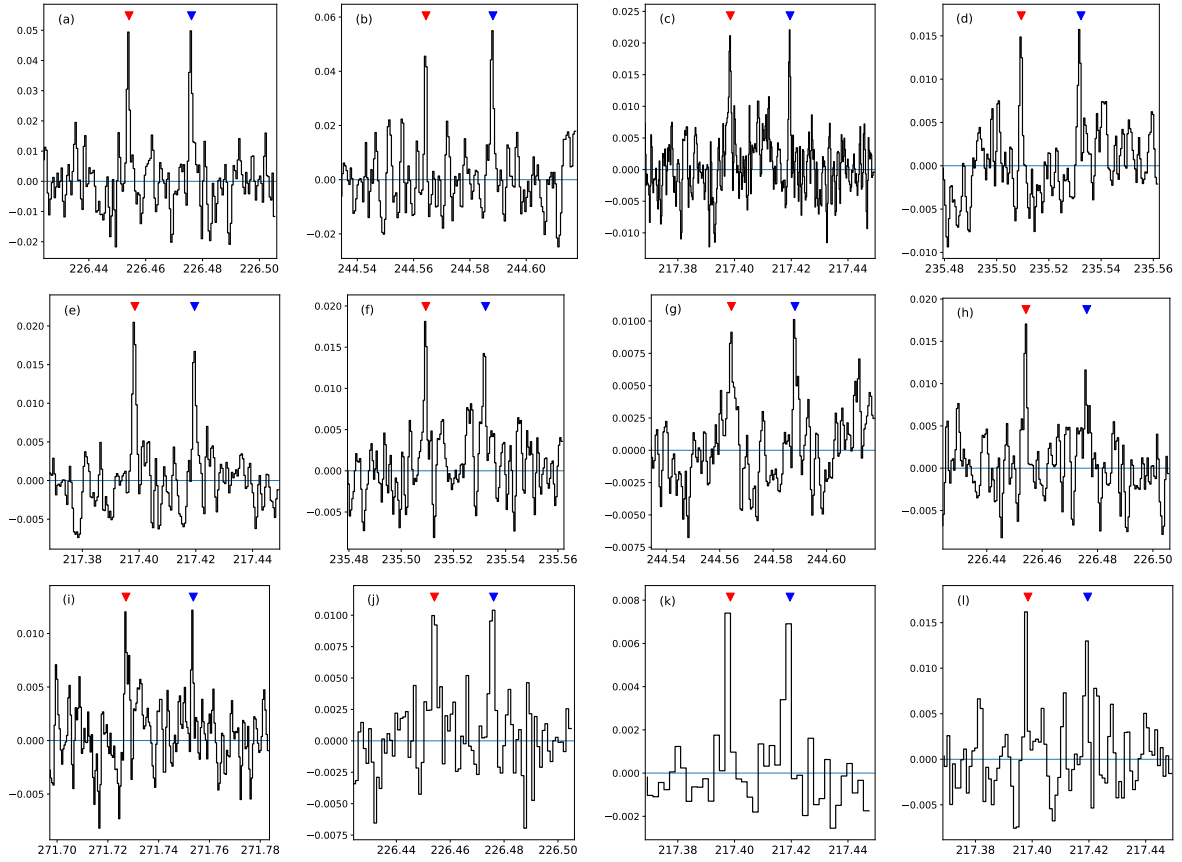


Figure 1. Spectra of HC^{13}CCN (red marker) and HCC^{13}CN (blue marker). X and Y axes are for rest frequency (GHz) and intensity (Jy/beam), respectively. Order of panel is corresponding to Table 1 from upper left to bottom right.

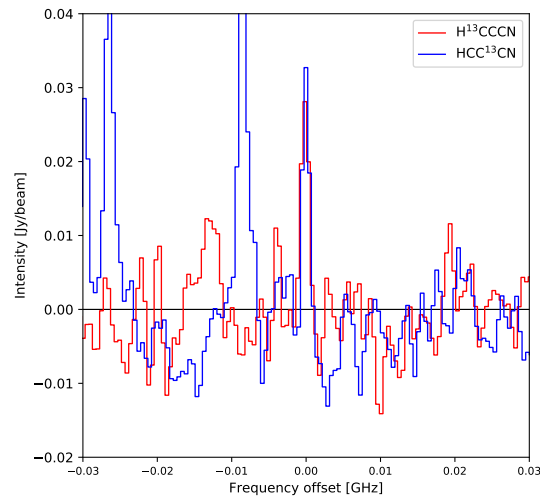


Figure 2. Over-plotted spectra of $\text{H}^{13}\text{CCCN}(J=35-34)$, red) and $\text{HCC}^{13}\text{CN}(J=34-33)$, blue). Two strong spectral lines shown in the left of HCC^{13}CN are $J=36-35$ transition group of $\text{C}_2\text{H}_5\text{CN}$. At the left edge, a $\text{HC}^{13}\text{CCN}(J = 34-33)$ line which is blended with one of $\text{C}_2\text{H}_5\text{CN}$ line is present.

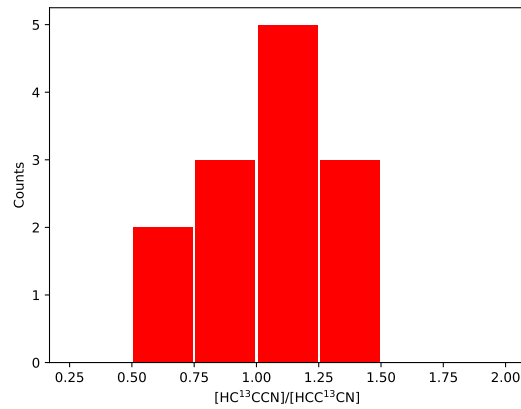


Figure 3. A histogram of derived $[\text{HC}^{13}\text{CCN}]/[\text{HCC}^{13}\text{CN}]$.

Table 1. Summary of observation parameters and result with error

Project code	Obs. date y-m-d	Obs. time (s)	Beam shape (")	Δf (kHz)	HC ¹³ CCN		HCC ¹³ CN		Abundance Ratio
					Freq. (GHz)	Integrated intensity (Jy/beam km/s)	Freq. (GHz)	Integrated intensity (Jy/beam km/s)	
(a) 2011.0.00735	2012-01-13	217.68	2.00×1.30	488	226.4541	0.0614(7.1)	226.4761	0.0712(8.2)	0.86(0.16)
(b) 2011.0.00735	2012-01-13	217.68	1.87×1.21	488	244.5644	0.0451(4.2)	244.5882	0.0726(6.8)	0.62(0.17)
(c) 2012.1.00932	2014-03-11	157.344	1.15×0.75	244	217.3985	0.0284(7.8)	217.4196	0.0196(5.4)	1.44(0.32)
(d) 2012.1.00248	2014-04-29	158.304	0.81×0.59	488	235.5094	0.0188(5.9)	235.5323	0.0199(6.2)	0.95(0.22)
(e) 2012.1.00248	2014-04-29	158.304	0.88×0.65	488	217.3985	0.0345(12.1)	217.4196	0.0251(8.8)	1.37(0.19)
(f) 2012.1.00248	2014-04-29	158.304	0.95×0.58	488	235.5094	0.0255(6.8)	235.5323	0.0216(5.8)	1.18(0.27)
(g) 2012.1.00453	2014-07-07	157.344	0.48×0.44	488	244.5644	0.0150(5.3)	244.5882	0.0125(4.1)	1.19(0.35)
(h) 2013.1.00271	2015-04-05	157.344	1.45×1.01	488	226.4541	0.0214(6.3)	226.4761	0.0161(4.7)	1.34(0.35)
(i) 2012.1.00453	2015-05-13	157.344	0.66×0.47	488	271.7271	0.0124(5.1)	271.7536	0.0104(4.3)	1.20(0.37)
(j) 2015.1.01312	2016-03-21	151.2	0.90×0.72	976	226.4541	0.0191(5.1)	226.4761	0.0172(5.3)	1.11(0.32)
(k) 2015.1.00512	2016-03-31	604.8	1.07×0.84	217.3985	0.0105(4.6)	217.4196	0.0143(6.3)	0.73(0.20)	
(l) 2015.1.00315	2016-04-02	755.0	1.09×0.84	976	217.3985	0.0199(4.3)	217.4196	0.0201(4.4)	1.00(0.32)
2012.1.00178	2015-04-22	157.344	1.19×0.74	488	H ¹³ CCCN		HCC ¹³ CN		
					308.5041	0.0293(8.4)	307.9689	0.0264(6.5)	1.17(0.20)

NOTE—Integrated intensities and abundance ratios are followed by 1- σ S/N ratio in parenthesis. Abundance ratios are expressed as [HC¹³CCN]/[HCC¹³CN] or [H¹³CCCN]/[HCC¹³CN].

REFERENCES

- Araki, M., Takano, S., Sakai, N., et al. 2016, *The Astrophysical Journal*, 833, 291. <http://stacks.iop.org/0004-637X/833/i=2/a=291?key=crossref.95e92a92026b0f84596ad0481bb8baa4>
- Colzi, L., Sipilä, O., Roueff, E., Caselli, P., & Fontani, F. 2020, *Astronomy & Astrophysics*, 640, A51. <https://www.aanda.org/10.1051/0004-6361/202038251>
- Cordiner, M. A., Nixon, C. A., Charnley, S. B., et al. 2018, *The Astrophysical Journal*, 859, L15. <http://stacks.iop.org/2041-8205/859/i=1/a=L15?key=crossref.3db3b0a1e328504fc7cc09382363bbb3>
- Cordiner, M. a., Remijan, a. J., Boissier, J., et al. 2014, *The Astrophysical Journal*, 792, L2. <http://stacks.iop.org/2041-8205/792/i=1/a=L2?key=crossref.ee2e6ee7802e4b0cce80f28370e91640>
- Cordiner, M. a., Palmer, M. Y., Nixon, C. a., et al. 2015, *The Astrophysical Journal*, 800, L14. <http://stacks.iop.org/2041-8205/800/i=1/a=L14?key=crossref.d304cda239aa0a7fa1c22fbf25847529>
- Cordiner, M. A., Palmer, M. Y., de Val-Borro, M., et al. 2019, *The Astrophysical Journal*, 870, L26. <http://dx.doi.org/10.3847/2041-8213/aafb05>
- Coustenis, A., Jennings, D. E., Achterberg, R. K., et al. 2018, *The Astrophysical Journal*, 854, L30. <http://dx.doi.org/10.3847/2041-8213/aaadbhttp://stacks.iop.org/2041-8205/854/i=2/a=L30?key=crossref.1fee7cb410afa4b45f2e8fba70342bf9>
- Coustenis, A., Salama, A., Schulz, B., et al. 2003, *Icarus*, 161, 383
- Coustenis, A., Salama, A., Lellouch, E., et al. 1998, *Astronomy and Astrophysics*, 336, 85
- Coustenis, A., Achterberg, R. K., Conrath, B. J., et al. 2007, *Icarus*, 189, 35
- Coustenis, a., Jennings, D. E., Nixon, C. a., et al. 2010, *Icarus*, 207, 461. <http://dx.doi.org/10.1016/j.icarus.2009.11.027>
- Coustenis, A., Jennings, D. E., Achterberg, R. K., et al. 2016, *Icarus*, 270, 409. <http://dx.doi.org/10.1016/j.icarus.2015.08.027>
- Furuya, K., Aikawa, Y., Sakai, N., & Yamamoto, S. 2011, *Astrophysical Journal*, 731, doi:10.1088/0004-637X/731/1/38
- Gurwell, M. a. 2004, *The Astrophysical Journal*, 616, L7
- Hidayat, T., Marten, a., Bézard, B., & Gautier, D. 1997, *Icarus*, 182, 170. <http://www.sciencedirect.com/science/article/pii/S0019103596956407>
- Iino, T., Mizuno, A., Nakajima, T., et al. 2014, *Planetary and Space Science*, 104, 211
- Iino, T., Sagawa, H., & Tsukagoshi, T. 2020, *The Astrophysical Journal*, 890, 95. <http://dx.doi.org/10.3847/1538-4357/ab66b0https://iopscience.iop.org/article/10.3847/1538-4357/ab66b0>
- Jennings, D. E., Nixon, C. A., Jolly, A., et al. 2008, *The Astrophysical Journal*, 681, L109. <http://iopscience.iop.org/article/10.1086/590534>
- Kunde, V. G., Aikin, A. C., Hanel, R. A., et al. 1981, *Nature*, 292, 686. <http://www.nature.com/doi/10.1038/292686a0http://www.nature.com/articles/292686a0>
- Lavvas, P., Coustenis, A., & Vardavas, I. 2008, *Planetary and Space Science*, 56, 67. <https://linkinghub.elsevier.com/retrieve/pii/S0032063307002292>
- Loison, J. C., Hébrard, E., Dobrijevic, M., et al. 2015, *Icarus*, 247, 218. <http://dx.doi.org/10.1016/j.icarus.2014.09.039>
- Loison, J. C., Wakelam, V., Gratier, P., & Hickson, K. M. 2020, *Monthly Notices of the Royal Astronomical Society*, 498, 4663
- Molter, E. M., Nixon, C. A., Cordiner, M. A., et al. 2016, *The Astronomical Journal*, 152, 42. <http://stacks.iop.org/1538-3881/152/i=2/a=42?key=crossref.4259a4ec01fd61a24d2bd0bf6ad0d077>
- Moreno, R., Lellouch, E., Lara, L. M., et al. 2011, *Astronomy & Astrophysics*, 536, L12. <http://www.aanda.org/10.1051/0004-6361/201118189>
- Nixon, C. A., Achterberg, R. K., Vinatier, S., et al. 2008, *Icarus*, 195, 778
- Nixon, C. a., Temelso, B., Vinatier, S., et al. 2012, *The Astrophysical Journal*, 749, 159

- Picket, H. M., Poynter, R. L., Cohen, E. A., et al. 1998, *Journal of Quantitative Spectroscopy and Radiative Transfer*, 60, 883.
<http://www.sciencedirect.com/science/article/pii/S0022407398000910><http://linkinghub.elsevier.com/retrieve/pii/S0022407398000910>
- Takano, S., Masuda, A., Hirahara, Y., et al. 1998, *Astronomy and Astrophysics*, 1169, 1156
- Taniguchi, K., Herbst, E., Ozeki, H., & Saito, M. 2019, *The Astrophysical Journal*, 884, 167.
<http://dx.doi.org/10.3847/1538-4357/ab3eb8>
- Taniguchi, K., Ozeki, H., & Saito, M. 2017, *The Astrophysical Journal*, 846, 46
- Taniguchi, K., Saito, M., & Ozeki, H. 2016, *The Astrophysical Journal*, 830, 106. <http://dx.doi.org/10.3847/0004-637X/830/2/106>
- Taniguchi, K., Herbst, E., Majumdar, L., et al. 2021, *The Astrophysical Journal*, 908, 100.
<https://iopscience.iop.org/article/10.3847/1538-4357/abd6c9>
- Thelen, A. E., Nixon, C. A., Chanover, N. J., et al. 2018, *Icarus*, 307, 380.
<https://doi.org/10.1016/j.icarus.2017.10.042>
- Thelen, A. E., Nixon, C., Chanover, N., et al. 2019, *Icarus*, 319, 417. <https://linkinghub.elsevier.com/retrieve/pii/S0019103518304184>
- Turner, B. E. 1991, *The Astrophysical Journal Supplement Series*, 76, 617.
<http://adsabs.harvard.edu/doi/10.1086/191577>
- Vuitton, V., Yelle, R., & McEwan, M. 2007, *Icarus*, 191, 722. <http://linkinghub.elsevier.com/retrieve/pii/S0019103507002709>
- Vuitton, V., Yelle, R. V., Klippenstein, S. J., Hörst, S. M., & Lavvas, P. 2019, *Icarus*, 324, 120.
<https://doi.org/10.1016/j.icarus.2018.06.013>